Widely tunable Q-switched dual-wavelength synchronous-pulsed Tm-doped fiber laser emitting in the 2 μm region

Mostafa Sabra, Baptiste Leconte, Romain Dauliat, Dia Darwich, Tobias Tiess, Anka Schwuchow, Raphaël Jamier, Georges Humbert, Katrin Wondraczek, Matthias Jäger, et al.

Widely tunable Q-switched dual-wavelength synchronous-pulsed Tm-doped fiber laser emitting in the 2 µm region

MOSTAFA SABRA,[1,*] BAPTISTE LECONTE,[1] ROMAIN DAULIAT,[1] DIA DARWICH,[1] TOBIAS TIESS,[2,] ANKA SCHWUCHOW,[2] RAPHAEL JAMIER,[1] GEORGES HUMBERT,[1] KATRIN WONDRACZEK,[2] MATTHIAS JÄGER[2,] AND PHILIPPE ROY[1]

[1]*Xlim Research Institute, UMR CNRS/University of Limoges, 123 Avenue Albert Thomas, 87060 Limoges, France*
[2]*Leibniz Institute of Photonic Technology, Albert-Einstein-Straße 9, 07745 Jena, Germany*
**Corresponding author: mostafa.sabra@xlim.fr*

Received XX Month XXXX; revised XX Month, XXXX; accepted XX Month XXXX; posted XX Month XXXX (Doc. ID XXXXX); published XX Month XXXX

We demonstrate a widely tunable Q-switched dual-wavelength fiber laser emitting synchronized pulses in the 2 µm spectral range. Owing to the use of a thulium doped rod-type Fully-Aperiodic Large Pitch Fiber (FA-LPF), together with an acousto-optic modulator (AOM), and two Volume Bragg Gratings (VBGs), the wavelength separation was shown to be continuously tunable from 1 nm to 120 nm (~0.1-10 THz). A peak power of more than 8 kW was demonstrated over the whole tuning range for a repetition rate of 1 KHz and a 26 ns pulse duration. The repetition rate was modulated from 1 kHz to 30 kHz, and the laser pulse duration measured between 23 ns and 130 ns, depending of the repetition rate and the wavelength separation. © 2018 Optical Society of America

OCIS codes: *(140.3600) Lasers, tunable; (060.3510) Lasers, fiber; (060.2310) Fiber optics; (060.4005) Microstructured fibers; (050.7330) Volume gratings; (140.3540) Lasers, Q-switched; (040.2235) Far infrared or terahertz.*

http://dx.doi.org/10.1364/OL.99.099999

The development of tunable dual-wavelength laser sources has recently attracted much attention in a broad range of application, such as nonlinear biomedical applications [1], atmospheric sensing [2], spectroscopic measurements [3] and distance measurements [4]. Such sources have also drawn some interest for realizing tunable terahertz (THz) sources, by difference frequency generation (DFG) in a nonlinear crystal [5, 6, 7].

The needs of dual-wavelength laser associating a wide tunability range of the spectral separation between both wavelengths ($\Delta\lambda$), a high peak power in the kW range, and narrow spectral laser peaks is thus triggered by these applications. All those properties are simultaneously accessible in the ns-regime by Q-switched laser.

Moreover, since fiber lasers offer numerous advantages compared to solid-state lasers, as excellent beam quality, high conversion efficiency, high average power, high thermal dissipation, and thermal stability, it stands out as an ideal candidate. Dual-wavelength fiber laser with fixed $\Delta\lambda$ have been realized by using two fiber lasers based on a pair of fiber Bragg gratings (FBGs) [8], or by associating two single-frequency fiber lasers [9].

A dual-wavelength fiber laser with a $\Delta\lambda$ tunability of 25 nm, around the wavelength of 1.07 µm, has been recently demonstrated by Tiess et al. [10]. This system is based on a delay line composed of a discretely chirped FBG array inserted in a theta cavity configuration. An AOM is used for generating synchronous pulses and selecting a specific couple of wavelengths by controlling the pulses delay in the FBG array. However, as others all-fiber dual-wavelength sources, the output power is limited by parasitic nonlinear effects and requires further amplification stages to obtain high peak powers in the kW range.

Laser configurations based on an active fiber as gain medium and free space AOM, offer possibility to broader the tunability range by using free-space components and reduce the parasitic nonlinear effects by using large mode area active-fiber. Kadwani et al. [11] have used a diffraction grating associated to a Tm-doped photonic crystal fiber for demonstrating a broad tunability of 200 nm (around 2 µm) into a single-wavelength laser with a maximum peak power of 6 kW (in nanosecond pulse regime). However, a diffraction grating is not suitable for tunable dual-wavelength laser operation since it is difficult to set two diffraction gratings in cascade. VBG component reflect the beam only at the Bragg wavelength enabling dual-wavelength reflections by cascading two VBGs. Furthermore, VBGs offer the advantages of narrow linewidth reflection, high reflectivity, high damage threshold, low insertion

losses, and continuous selection of the reflected wavelength by rotation. Dual-wavelength fiber laser with a tunability range of $\Delta\lambda$ from 1 nm to 144 nm has recently been demonstrated by cascading a pair of VBGs [12].

In this letter, a widely tunable Q-switched dual-wavelength pulsed fiber laser based on the association of two VBGs, a free space AOM and a rod-type Tm-doped FA-LPF is achieved. The laser emission in the 2 µm range is selected for this demonstration since this domain is more favorable for applications based on nonlinear crystals (as DFG of THz waves [5, 7]), due to a larger quantum efficiency in this frequency range. The tuning range of dual wavelength separation from $\Delta\lambda = 1$ nm to 120 nm is to the best of our knowledge the widest reported in such a fiber-based laser system. Synchronous pulses with duration of 26 ns and peak power > 8 kW, for a repetition rate of 1 kHz have been generated over the whole tuning range. Such kW peak power level has been made accessible by the first use of a Tm-doped rod-type FA-LPF.

The experimental setup is illustrated in Fig. 1. A novel 62 cm long Tm-doped rod-type FA-LPF, angle cleaved end facet (5°) on the pumping side to avoid parasitic optical feedback, is used. The fiber was placed on a metal plate with thermal paste applied all along the fiber to dissipate the heat. An AOM (Gooch & Housego) controlled by a radio frequency signal was used to modulate the losses in the laser cavity, with > 80% of diffraction efficiency on the first order and a rise time of 40 ns. Two VBGs (VBG1 and VBG2, from OptiGrate Corp., dimensions of 5x5x5 mm) with high reflectivity (>90%), centered at 1984 nm and 1970 nm respectively, were used as spectral filters to select the emitting wavelengths of the laser.

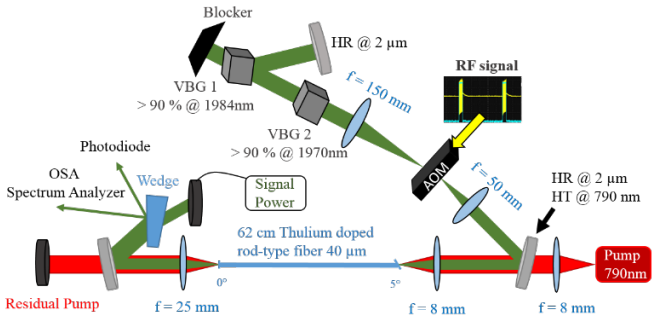

Fig. 1. Experimental setup of the Q-switched tunable dual-wavelength Tm-doped fiber.

The laser cavity is formed on one side by the two VBGs, and on the other side by the 4% Fresnel reflection of the perpendicularly cleaved fiber end facet, corresponding to the output coupler. The fiber was pumped at 790 nm by a multimode fibred laser diode (core diameter of 105 µm and NA of 0.22), providing up to 31 W output power. Two dichroic mirrors with high reflectivity at 2 µm and high transmission at 790 nm, were used to reflect the signal in the direction of the VBGs (while transmitting the pump), and to separate the residual pump power from the output signal. A lens with a focal length of 150 mm is used to properly collimate the beam onto the VBGs, essential to benefit from their maximum reflectivity.

The Tm-doped rod-type FA-LPF has been specially devised to reduce nonlinear disturbances in pulsed operation and to increase the peak power. The design of this original fiber, shown in Fig. 2(a), is composed of a large Tm-doped core (in red) surrounded by an aperiodic pattern of low-index inclusions (in yellow) embedded into an index-matched passively doped silica cladding. This specific pattern ensures the confinement of the fundamental mode into the fiber core and the delocalization of high-order modes, even for very large core diameters [13]. A microscopic image of the fabricated fiber is presented in Fig.2 (b). The FA-LPF has a core diameter of 40 µm and an air-cladding diameter of 150 µm. The low-index inclusions has a diameter of 10 µm, and composed of fluorine-doped silica. The large mode field diameter (MFD) of 35 µm and the relative short fiber length of 62 cm are chosen to reduce the nonlinear effects and the ASE in the laser cavity.

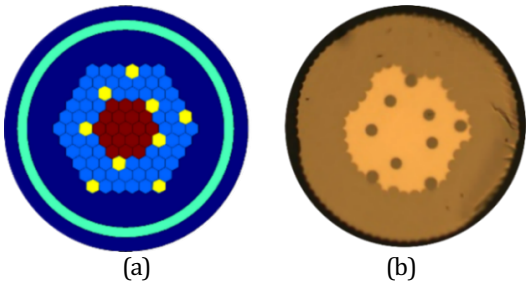

Fig. 2. (a) Schematic cross section of the reduced cladding FA-LPF design. The Tm-doped core is represented in red, the clear blue region corresponds to the index matched aluminum-doped silica material, the yellow hexagons stand for the low-index inclusions, the dark blue area is made of pure silica, and the green ring represents the air-cladding ensuring a high pump coupling efficiency. (b) Cross section picture taken with an optical microscope of the fabricated Tm-doped rod-type FA-LPF [14].

First tests have been realized for $\Delta\lambda = 3.8$ nm at different Repetition Rate (RR) from 1 kHz to 30 kHz, and at fixed pump power of 26.4 W. The output spectrum, temporal signal and average power of the laser at RR = 1 kHz have been measured respectively with an optical spectrum analyzer (OSA), a photodiode and a power-meter after a wedge, as shown in Fig. 1. The output spectrum is composed of two main laser peaks and two parasitic side peaks, each ones spaced by 3.8 nm (Fig. 3(a)). The linewidth at the full widths at half-maximum (FWHM) of each main laser peak is around 0.3 nm (the resolution of the OSA being 0.05 nm), and the signal contrast to the side lobes is about 21 dB. These parasitic peaks are the signature of the $\chi 3$ nonlinear four-wave-mixing (FWM) effect that appears when the phase of both laser peaks are nearly phase matched (i.e. at low $\Delta\lambda$) [10, 15]. As shown in Fig. 3(b), the pulse shape is Gaussian with a pulse duration of 25 ns. This temporal trace confirms the synchronization of the dual-wavelength pulses, without competition between the two pulses of the laser. It is worth noting that the distance between VBG2 and the high reflection mirror used to reflect the wavelength of VBG1 is shorter than 15 cm, thus yielding into negligible temporal difference between both pulses (<1 ns).

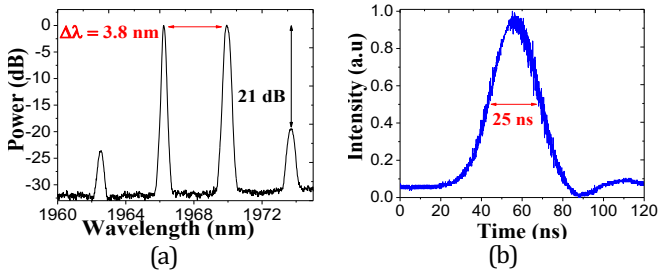

Fig. 3. (a) Output spectrum and (b) temporal trace measured at $\Delta\lambda = 3.8$ nm, pump power = 26.4 W and RR = 1 kHz.

The evolution of the output average power and peak power versus the RR is shown in Fig. 4. The peak power was calculated for each RR value, from the measured average power, the pulse width, and by subtracting the ASE power (7 mW) emitted by the Tm-doped rod-type FA-LPF. This former value was obtained by measuring the ASE power emitted by the rod-type fiber, pumped at 26.4 W in absence of seed power. As expected in Q-switched operation, lower RR increases the peak power and reduces the average power due to the high population inversion in the gain medium of the laser [16]. A maximum peak power of 11.9 kW and an average power of 0.3 W was obtained for RR = 1 kHz. The peak power was limited by the saturation of the population inversion for RR<1 kHz.

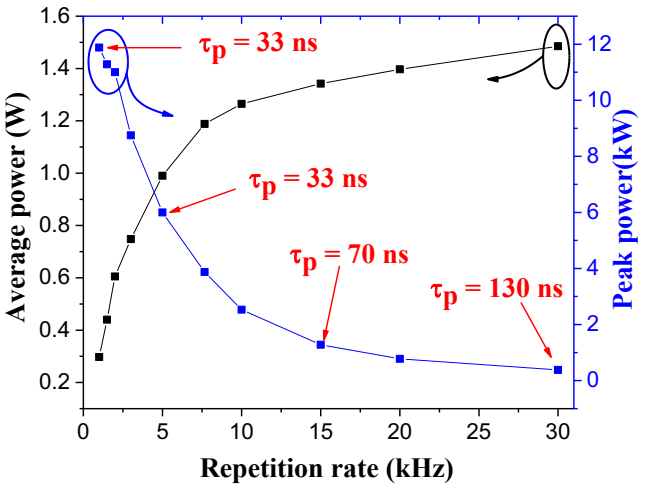

Fig. 4. Evolution of the average power and peak power (for Δλ = 3.8 nm and a pump power = 26.4 W) versus RR. Pulse duration values (τ_p) are written in red.

The tunability of Δλ was realized by changing the angle between the VBG1 and the signal beam, referring to the Bragg law:

$$\lambda_{(\theta)} = \lambda_{(\theta=0)} \cos(\theta)$$

Where $\lambda_{(\theta=0)}$ is the reflected wavelength at normal incidence (i.e. 1984 nm and 1970 nm, respectively for VBG1 and VBG2), and θ is the angle of incidence. VBG2 was set at normal angle of incidence. VGB1 was rotated to tune the reflected wavelength toward smaller wavelengths down to 1850 nm, leading to a wavelength separation up to 120 nm. By rotating VBG1 the signal beam was reflected with an angle depending of the incidence angle (θ). A high reflection mirror at 2 µm was used and rotated jointly with VBG1 to close the laser cavity over the reflected wavelength ($\lambda_{(\theta)}$). Output spectra obtained at different wavelength separation from Δλ = 15 nm to Δλ =120 nm are shown in Fig. 5. The signal to noise ratio is higher than 30 dB and the parasitic peaks from FWM effect are suppressed above Δλ = 45 nm. It is worth noting that Δλ was limited to 120 nm by the power drop due to low emission cross section for smaller wavelength (λ<1850 nm, i.e. Δλ > 120 nm). The pulse durations and peak powers, measured at RR = 1 kHz, are below 30 ns and above 8 kW, respectively (Fig. 6). The maximum peak power of 13.5 kW was obtained at Δλ = 15 nm with a pulse duration of 24.5 ns, corresponding to a pulse energy of 0.33 mJ. Although spectrum clearly show laser lines due to FWM, their contribution is neglected as their level is 21dB smaller than the main laser lines. The variations in peak power and pulse duration are logically influenced by the spectral profile of the gain of the Tm-doped fiber and the slight reduction of the VBG reflectivity with the rotating angle (θ).

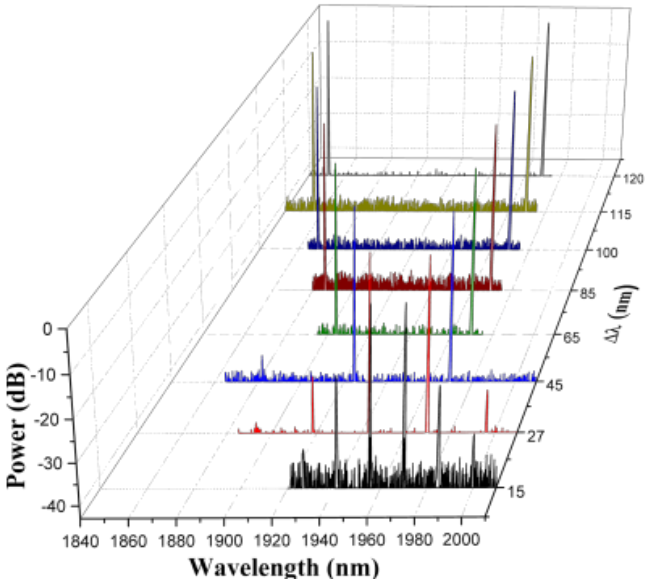

Fig. 5. Spectra of Q-switched dual-wavelength emissions at different wavelength separation (Δλ) from 15 nm to 120 nm.

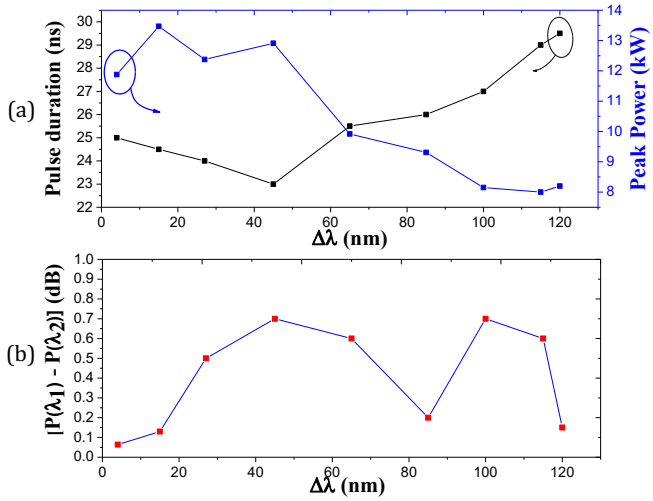

Fig. 6. (a) Measured output peak power and pulse duration, and (b) the output power difference of both wavelengths emitted [P(λ1 – P(λ2)], versus Δλ from 15 nm to 120 nm (RR = 1 kHz, pump power = 26.4 W)

Measurements at RR = 1 kHz of different Δλ showed no significant power difference between both wavelengths (as shown in Fig.6 (b)), without temporal instability. Besides, as for Δλ = 3.8 nm (fig. 3(a)), no competition between both pulses was observed for larger Δλ, over the whole tuning range. For example, the measured pulse profiles at Δλ = 85 nm and Δλ = 115 nm (Fig. 7) have a Gaussian shape with a FWHM of 26 ns and 29 ns, respectively. Nevertheless, parasitic instabilities appear at RR > 10 kHz and Δλ > 65 nm, when competitions between both wavelengths appears due to a weaker population inversion at high RR and to a large difference of emission cross-sections at large Δλ. It is worth noting that the optimization of the position of the whole tuning range on the gain spectrum would limit further this regime of instabilities.

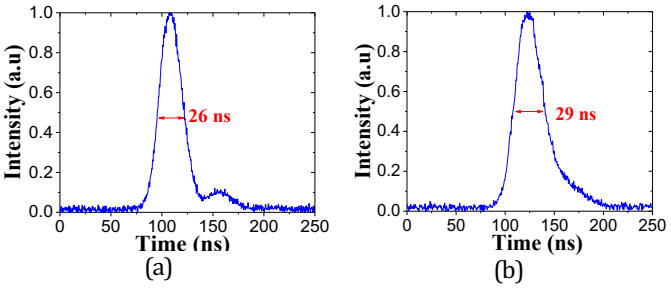

Fig. 7. Temporal traces measured at 26.4 W of pump power for different wavelength separation of Δλ = 85 nm (a), and Δλ = 115 nm (b).

The measured slope efficiencies of the average output power of the laser were 7.15%, 12%, and 13%, at RR = 3 kHz, 7.5 kHz, and 30 kHz, respectively (Fig.8). The wavelength separation was set to Δλ = 25 nm. As expected, the average power increases with RR from 0.97 W at 3 kHz to 1.87 W at 30 kHz due to the high overall inversion. A picture of the signal beam profile measured at the output of the laser cavity after the wedge (Fig.1) presented in the inset of Fig. 8 has a Gaussian shape. The beam profile was slightly distorted due to parasitic astigmatism in the collimation system.

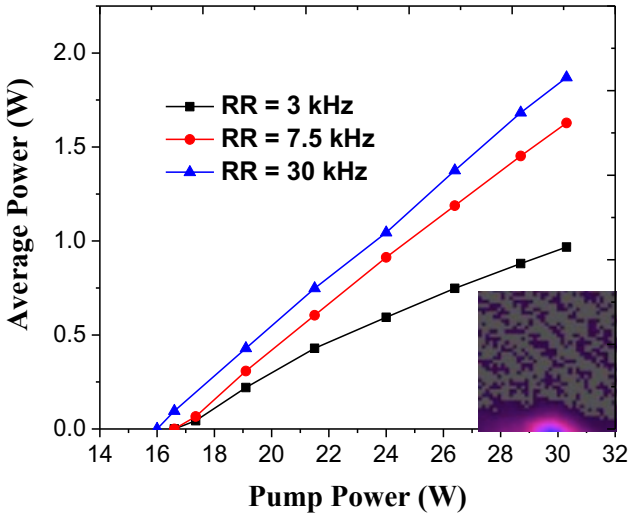

Fig. 8. Evolution of the average power versus the pump power for different RR of 3 kHz, 7.5 kHz, and 30 kHz. Insert, measured power distribution of the signal beam (at RR = 7.5 kHz and pump power = 26.4 W, corresponding to an output power of 1.9 W).

In conclusion, a wide continuously tunable Q-switched dual-wavelength thulium-doped fiber laser is demonstrated, using two VBGs and a free space AOM together for the first time to our knowledge. A novel design of thulium doped fiber (FA-LPF) was presented and used, to reduce the nonlinear effects in the laser cavity. A peak power higher than 8 kW, with a signal to noise contrast >20 dB, covering the tuning range from 1nm to 120 nm of wavelength separation have been achieved. The highest peak power was obtained at 15 nm of wavelength separation (13.5 kW), corresponding to a pulse duration of 24.5 ns at 1 kHz of RR. This configuration is well adapted to realize a tunable THz source by DFG by using a nonlinear crystal directly after the output signal, or by boosting the signal in an amplification stage to increase the peak power levels.

Funding. French Research Agency (ANR) (ANR-15 CE24-0031-01); German Research Foundation (DFG) (DFG GZ JA 2611/1-1).

Acknowledgment. We thank the COST MP1401 for supporting this work, and Kay Schuster for his technical support of the project.

References

1. T. Gottschall, T. Meyer, M. Schmitt, J. Popp, J. Limpert, and A. Tünnermann, Opt. Express **23**, 23968-23977 (2015).
2. U. Sharma, C.-S. Kim, J. U. Kang, and N. M. Fried, in *Laser Applications to Chemical and Environmental Analysis 2004* (Optical Society of America, 2004), p. MB3.
3. R. Gaulton, F. Danson, F. Ramirez, and O. Gunawan, Remote. Sens. Environ. **132**, 32-39 (2013).
4. B. Lin, X. Zhao, M. He, Y. Pan, J. Chen, S. Cao, Y. Lin, Q. Wang, Z. Zheng and Z. Fang, IEEE Photonics Journal **9**, 2017.
5. D. Yan, Y. Wang, D. Xu, P. Liu, C. Yan, J. Shi, H. Liu, Y. He, L. Tang, J. Feng, J. Guo, W. Shi, K. Zhong, Y. H. Tsang, and J. Yao, Photon. Res. **5**, 82-87 (2017).
6. M. Y. Jeon, N. Kim, J. Shin, J. S. Jeong, S.-P. Han, C. W. Lee, Y. A. Leem, D. S. Yee, H. S. Chun, and K. H. Park, Opt. Express **18**, 12291-12297 (2010).
7. J. Mei, K. Zhong, M. Wang, Y. Liu, D. Xu, W. Shi, Y. Wang, J. Yao, R. A. Norwood, and N. Peyghambarian, Opt. Express **24**, 23368-23375 (2016).
8. W. Shi, M. Leigh, J. Zong, and Shibin Jiang, Opt. Lett. **32**, 949-951 (2007).
9. M. A. Leigh, W. Shi, J. Zong, Z. Yao, S. Jiang, and N. Peyghambarian, Photonics Tech. Lett. **21**, 27-29 (2009).
10. T. Tiess, M. Becker, M. Rothhardt, H. Bartelt and M. Jäger, Opt. Express **25**, 26393-26404 (2017).
11. P. Kadwani, N. Modsching, R. A. Sims, L. Leick, J. Broeng, L. Shah, and M. Richardson, Opt. Lett. **37**, 1664-1666 (2012).
12. M. Sabra, B. Leconte, D. Darwich, R. Dauliat, T. Tiess, R. Jamier, G. Humbert, M. Jaer, K. Schuster and P. Roy, Journal of Lightwave Tech. **37**, 2307-2310 (2019).
13. M. A. Malleville, R. Dauliat, A. Benoît, B. Leconte, D. Darwich, R. D. Jeu, R. Jamier, K. Schuster, and P. Roy, Opt. Lett. **42**, 5230-5233 (2017).
14. D. Darwich, B. Leconte, R. Dauliat, M. Sabra, R. du Jeu, M. A. Malleville, R. Jamier, F. Gutty, C. Larat, E. Lallier, K. Schuster, and P. Roy, in *Advanced Photonics congress 2018* (Optical Society of America, 2018).
15. S. Song, C. T. Allen, K. R. Demarest, and R.Hui, Journal of Lightwave Tech. **17**, 2285-2290 (1999).
16. M. Eichhorn, and D. Jackson, Opt. Lett. **32**, 2780-2782 (2007).